Liqun Xie, Tingan Zhang*, Guozhi Lv, Jinlin Yang and Yanxiu Wang

The effect of NaOH on the direct calcification–carbonation method for processing of Bayer process red mud

https://doi.org/10.1515/gps-2017-0070
Received May 8, 2017; accepted October 13, 2017; previously published online December 6, 2017

Abstract: The Bayer red mud generated from the alumina industry is a hazardous solid waste. In our team, a green calcification–carbonation process is proposed for its disposal. Red mud is treated with lime to convert the silicon phase in solution into hydrogarnet, which is then decomposed by CO_2 to recover alumina. In order to simplify the process flow, the direct carbonation process is employed, in which the NaOH-containing solution resulting from calcification is sent directly to carbonation without prior liquid–solid separation. The discrete and direct carbonation processes gave 34.9% and 35.5% alumina recoveries, respectively, with Na_2O contents in the final red muds of 0.15 %wt and 0.21 %wt, respectively. The optimum NaOH concentration in the whole calcification–carbonation process liquor was 40 g/l. Under this alkali condition, alumina recovery reached 40.5% and the Na_2O content in the processed red mud was reduced to <1 %wt.

Keywords: alkali; calcification–carbonation; direct process; hydrogarnet; red mud.

1 Introduction

The accumulation of red mud, a solid waste because of its high alkalinity discharged from alumina production by the Bayer process, has become a worldwide concern [1]. The production of 1 ton of alumina results in about 1.0–1.5 tons of red mud, depending on the original bauxite properties and the efficiency of alumina digestion [2, 3]. At present, the global accumulation of red mud is estimated to be more than 2.7 billion tons and is rising at a rate of 1.20×10^8 ton/year [4]. The most widely used current method is dam stockpiling. However, this method is limited by high maintenance costs and large footprint [5]. Alternative methods of disposal and utilization of red mud have therefore attracted significant research attention.

During the past several decades, research concerning treatment of Bayer process red mud has focused on three main aspects [6]: (1) environmental disposal (e.g. effluent handling [7] and placement in landfills [8]); (2) its use in materials (e.g. ceramics [9] and cement [10]); and (3) metallurgical uses (e.g. reuse of the Fe, Al, Ti and Na components [2, 11–13]). The above applications are restricted by their process efficiencies, volume, costs and mud-associated risks. Despite advances in addressing treatment of bauxite residues, there are only a few successful implementations, attributed to good local markets and economic conditions; many applications have failed due to high costs and low yields.

In the Bayer process, most of the aluminum in bauxite is converted into the sodium aluminate in the solution, and the silicon phase is converted into hydrated sodium aluminosilicate in the red mud. The reaction of the digestion process is as follows:

$$Al_2O_3\cdot 2SiO_2\cdot 2H_2O + 6NaOH \rightarrow 2Na_2SiO_3 + 2NaAl(OH)_4 + H_2O \quad (1)$$

$$xNa_2SiO_3 + 2NaAl(OH)_4 + (2-x)H_2O \rightarrow Na_2O\cdot Al_2O_3\cdot xSiO_2\cdot(6-2x)H_2O + 2xNaOH\ (x=1.7\sim2) \quad (2)$$

The equilibrium structure of the red mud produced by the Bayer is $Na_2O\cdot Al_2O_3\cdot xSiO_2\cdot(6-2x)H_2O$ ($x=1.7\sim2$), and the theoretical alumina to silica ratio (A/S) is 1 (A/S for most of the actual red mud is 1.3–1.4).

Our team has proposed a novel calcification–carbonation method [14–18] for disposal of Bayer process red mud. Red mud is treated with lime to convert the silicon phase in solution into hydrogarnet [19–21]:

$$Na_2O\cdot Al_2O_3\cdot xSiO_2\cdot(6-2x)H_2O + 3CaO + H_2O \rightarrow 3CaO\cdot Al_2O_3\cdot xSiO_2\cdot(6-2x)H_2O + 2NaOH \quad (3)$$

***Corresponding author: Tingan Zhang,** Key Laboratory of Ecological Metallurgy of Multi-metal Intergrown Ores, Ministry of Education, School of Metallurgy, Northeastern University, Shenyang 110004, China, e-mail: zta2000@163.net
Liqun Xie, Guozhi Lv, Jinlin Yang and Yanxiu Wang: Key Laboratory of Ecological Metallurgy of Multi-metal Intergrown Ores, Ministry of Education, School of Metallurgy, Northeastern University, Shenyang 110004, China

which is then decomposed by CO_2 to recover alumina:

$$3CaO{\cdot}Al_2O_3{\cdot}xSiO_2{\cdot}(6-2x)H_2O+(3-2x)CO_2 \rightarrow xCa_2SiO_4 + (3-2x)CaCO_3+2Al(OH)_3+(3-2x)H_2O. \quad (4)$$

In this study, we adopted the direct carbonation process to treat the calcification product, i.e. the slurry generated from calcification was not subjected to separation of solid hydrogarnet from the NaOH-containing solution, but was sent directly to carbonation. This significantly simplifies the process flow sheet, promotes carbonation, improves its efficiency and rate [22, 23], and reduces the energy consumption and costs of red mud disposal, enabling Bayer process red mud to be disposed of in a low-cost and harmless way.

2 Materials and methods

2.1 Direct calcification–carbonation process

We adopted the direct carbonation process to handle Bayer process red mud, in which the solution from calcification (adjusted to the appropriate carbonation temperature), without liquid–solid separation, was sent directly to carbonation, thereby significantly simplifying the production process. This differs from the discrete calcification–carbonation process in that NaOH present in solution after calcification enters the carbonation process. The effect of NaOH should therefore be studied. A simplified flow sheet for the direct calcification–carbonation method for red mud treatment is shown in Figure 1.

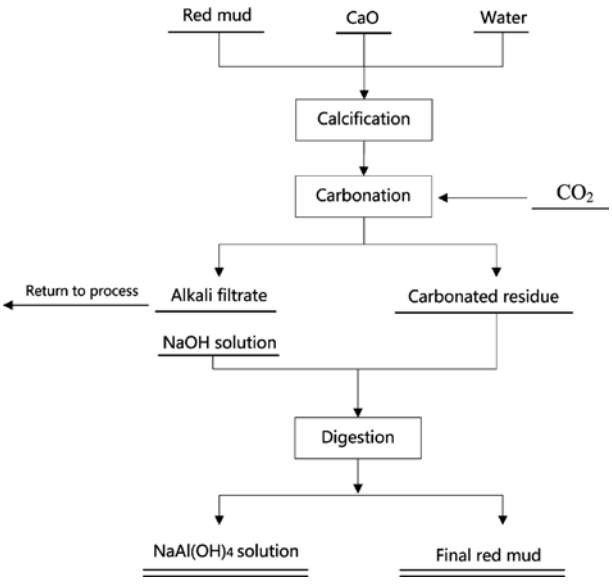

Figure 1: Flow sheet for proposed direct calcification–carbonation method.

2.2 Experimental method

The procedure consists of three steps: (1) calcification for canceling alkali out; (2) carbonation for decomposing the calcified residue; and (3) digestion of carbonated residue to recover alumina (Figure 2).

The calcification experiments were conducted in a 1 l stainless steel autoclave (Zhenwei Chemical Machinery Co. Ltd., Weihai, Shandong Province, China) (Figure 2) equipped with a magnetic stirrer and a proportional-integral-derivative temperature controller. A mixture of distilled water and 50 g red mud were added to the autoclave. After the temperature rose to 160°C, a certain amount of CaO milk was injected via the inflation inlet. The entire liquid-to-solid mass ratio was maintained at 5:1, Ca:Si molar ratio of 2.5:1; the reaction time was 1 h and stirring speed 300 r/min.

The carbonation experiments were also carried out in the autoclave. Distilled water and calcified residue at a mass ratio of 5:1 were added inside and reacted for 1 h under CO_2 conditions. Specifically: (1) at normal pressure, the autoclave was filled with CO_2 for 3 min at a rate of 20 ml/min so as to expel the air in advance; and (2) at elevated pressure, the calcified residue was carbonated under CO_2 atmosphere and pressure of 1.2 MPa, with a reaction time of 1 h and stirring speed of 300 r/min.

The direct experimental process is similar to the discrete process. After the calcification reaction, temperature inside the autoclave was adjusted to the carbonation temperature, and then CO_2 was passed into the autoclave. Namely, the solutions after calcification, without solid-liquid separation, were directly sent to carbonation, which largely simplified the production flow.

To isolate Al_2O_3 from the carbonated red mud and assess the effect of carbonation, we carried out parallel experiments in a water bath containing a mechanical agitator at a rate of 300 r/min. The carbonated residue was leached at 60°C for 1.5 h in the 100 g/l NaOH

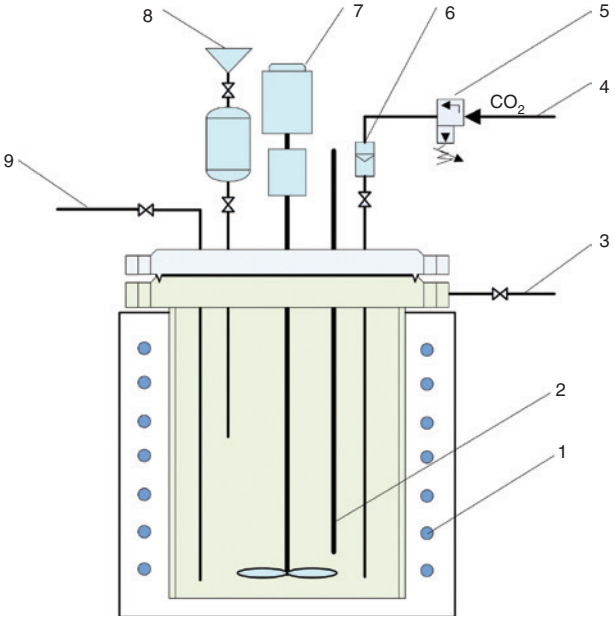

Figure 2: Schematic of the autoclave: 1, resistance wire; 2, thermocouple; 3, gas vent; 4, gas inlet; 5, pressure-release valve; 6, rotameter; 7, magnetic stirrer; 8, inflation inlet; 9, sample connection.

solution at a liquid-to-solid ratio of 10:1. After digestion, the slurry was filtered and washed.

2.3 Raw materials

Red mud (Zhengzhou Aluminum Company, Henan Province, China) was produced by the Bayer process by digestion of gibbsite bauxite. The chemical compositions of the raw red mud are shown in Table 1. It can be seen that the red mud was mainly composed of Al_2O_3 (22.20 %wt), SiO_2 (21.30 %wt), Na_2O (6.70 %wt), and CaO (11.43 %wt). The X-ray diffraction pattern of the red mud is shown in Figure 3, and the identified mineral phases were cancrinite [$Na_6Ca_{1.5}Al_6Si_6O_{24}(CO_3)_{1.6}$], gmelinite [$NaAl(SiO_3)_2{\cdot}3H_2O$], hydrogarnet [$Ca_3Al_2(SiO_4)_{1.25}(OH)_7$] and hematite ($Fe_2O_3$). NaOH and CaO used here were of analytical grade (Sinopharm Chemical Reagent Co. Ltd., China) and CO_2 with purity >99% was supplied from a 40 l gas cylinder (Kejin Chemical Gas Co. Ltd., Shenyang, China).

2.4 Analyses of solid sample

The compositions of the solid samples were detected on an X-ray fluorescence spectrometer (ZSX100e, Rigaku, Japan). Their mineralogical characteristics were recorded on a XRD meter (D8 Advance XRD, Bruker Company, Germany) with Cu Kα X-ray and at 40 kV, 40 mA and increment of 0.0095°. The morphologies of the samples were detected by scanning electron microscopy (SIGMA 500, Zeiss, Germany).

The recovery efficiency of alumina from red mud was expressed as follows:

$$\eta = \frac{(A/S)_0 - (A/S)_R}{(A/S)_0} \times 100\%,$$

where η is the actual withdrawal rate of Al_2O_3, %, and $(A/S)_0$ and $(A/S)_R$ are the mass ratios of Al_2O_3/SiO_2 in the original and final red muds, respectively.

Table 1: Chemical composition of red mud (%wt).

Al_2O_3	SiO_2	CaO	Fe_2O_3	Na_2O	TiO_2	L.O.I
22.20	21.30	11.43	16.31	6.70	3.26	12.92

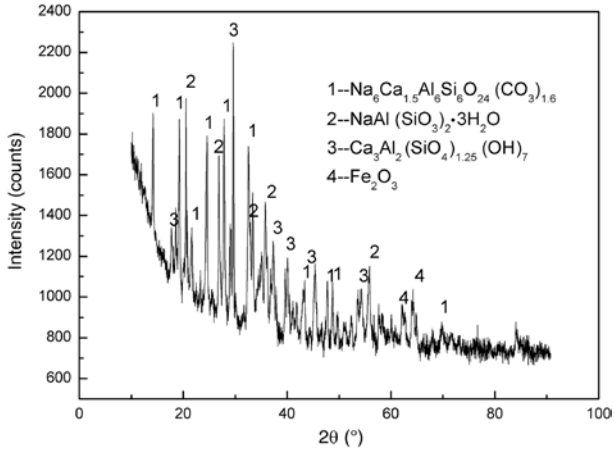

Figure 3: X-ray diffractogram of red mud used in experiments.

3 Results and discussion

3.1 Comparison between discrete and direct processes

To explore the feasibility of the direct carbonation process, we experimentally compared this with the discrete process. The optimum calcification conditions were as follows: reaction temperature of 160°C, Ca:Si molar ratio of 2.5:1, and liquid–solid ratio of 5:1. The optimum carbonation conditions were as follows: liquid–solid ratio of 5:1, pressure of 1.2 MPa, and the reaction temperature of 120°C.

Table 2 shows that both Al_2O_3 recovery and Na_2O concentrations were similar for the discrete and direct processes: the Al_2O_3 recoveries were maximized at 34.9% and 35.5%, respectively; the final Na_2O concentrations in the red mud were 0.15 %wt and 0.21 %wt, respectively. These findings suggested that the presence of residual NaOH when using the direct method without solid–liquid separation did not significantly affect the final results.

Figure 4 shows X-ray diffraction (XRD) patterns of the carbonated residues produced from the two processes. The phases identified in the product from the discrete process were fully consistent with that of the direct process. The carbonated residues contained unreacted hydrogarnet, calcium silicate, and calcium carbonate. The $Al(OH)_3$ phases are not probed by the XRD patterns, because of low crystallinity of the generated products [24].

Table 2: Comparison of the discrete and direct processes with respect to alumina recovery and Na_2O contents in the final red muds.

Method	Al_2O_3 (%wt)	SiO_2 (%wt)	Na_2O (%wt)	A/S	Al_2O_3 recovery (%)
Raw red mud	22.20	21.30	6.70	1.04	–
Discrete	9.73	14.31	0.17	0.68	34.6
Direct	9.65	14.40	0.23	0.67	35.6

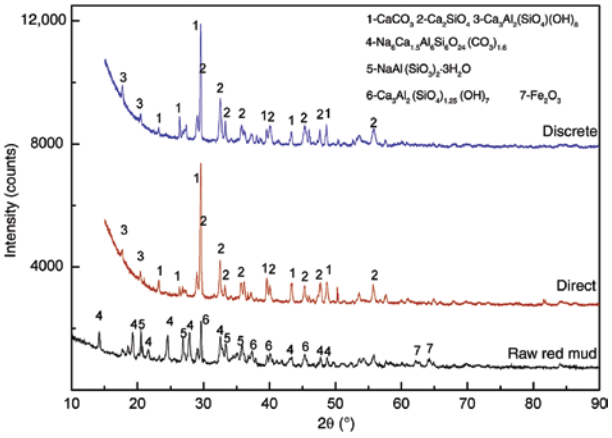

Figure 4: X-ray diffractogram of carbonated residues produced from the discrete and direct processes; X-ray diffractogram of raw red mud.

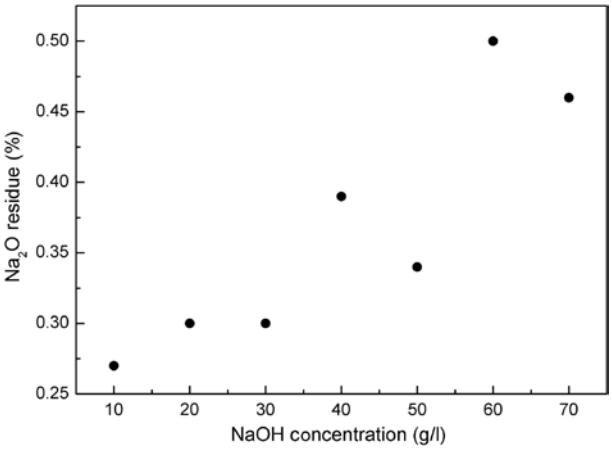

Figure 5: Na_2O content in calcified residues using NaOH solutions of different concentrations.

3.2 The effect of NaOH in the calcification process

The alkali will be enriched in industrial production. To simulate industrialization, different concentrations of NaOH solution were mixed with red mud and CaO in the reactor to investigate the effect of NaOH concentration on the whole process. The concentration of NaOH solution was divided into 10–70 g/l.

The calcification process was CaO instead of Na_2O in sodium aluminosilicate. The effect of different concentrations of NaOH solution on the calcification process was investigated by using the Na content in the calcified residue and XRD.

As can be seen from the calcification reaction, NaOH as a product may inhibit the positive progress of the reaction, but in fact the solubility of NaOH in water is very high, especially under high temperature conditions. Figure 5 shows that the increment of Na_2O in the calcified residues was not very obvious (0.27–0.5%wt). Figure 6 shows that the XRD patterns of residues calcified at various NaOH conditions are also very similar. The calcified residues included hydrogarnet [$Ca_3Al_2(SiO_4)(OH)_8$] and $CaCO_3$. The detected $CaCO_3$ is generated by unreacted CaO carbonated by CO_2 during filtering and drying.

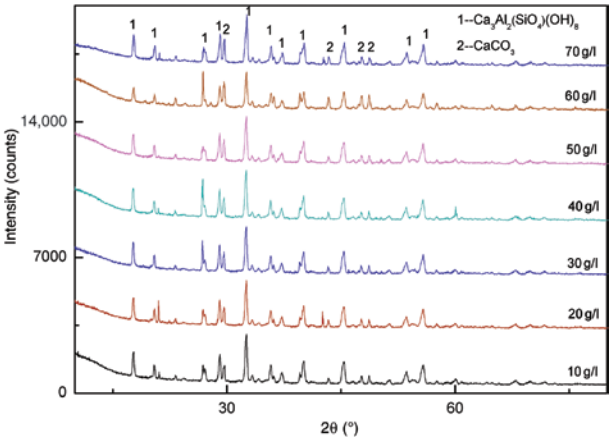

Figure 6: X-ray diffractograms of calcified residues produced from NaOH solutions of different concentrations.

3.3 The effect of NaOH on the carbonation process

The solutions from calcification (adjusted to the appropriate carbonation temperature), without liquid–solid separation, were sent directly to carbonation. The results are shown in Figures 7 and 8.

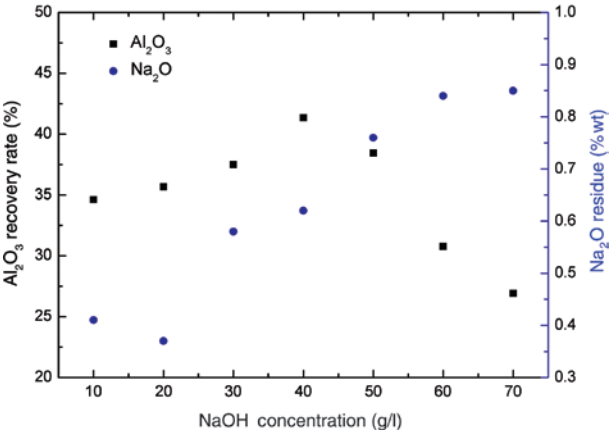

Figure 7: Analysis of final residues produced from the direct process using NaOH solutions of different concentrations.

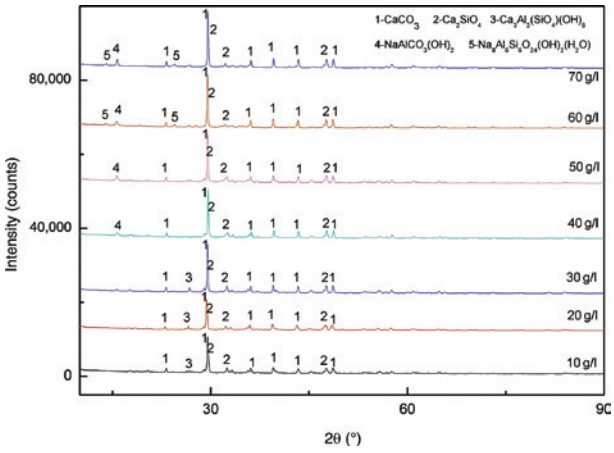

Figure 8: X-ray diffractograms of carbonated residues produced from NaOH solutions of different concentrations.

The final alumina recovery from the red mud first increased and then dropped as the NaOH concentration increased. Maximum recovery of 40.5% was achieved at a concentration of 40 g/l NaOH, which was better than those of both the direct (35.5%) and discrete (34.9%) processes. In contrast, the Na_2O concentration in the residues increased with increasing NaOH concentration. The Na_2O content was 0.6 %wt at 40 g/l NaOH addition, which was slightly higher than the discrete (0.15 %wt) process. These results suggested that appropriate addition of alkali can promote the decomposition of hydrogarnet and its reaction with $NaCO_3$; more Na moves from the solution into the residue, improving the alumina recovery and raising the Na concentration in the final product.

We analyzed the phases present in the carbonated residues and identified the effect of changing red mud composition. Figure 5 shows the XRD patterns of carbonated residues produced with addition of 10–70 g/l NaOH solutions.

At low NaOH concentrations (≤30 g/l), the hydrogarnet phase was not carbonated in the residues, but as the NaOH concentration increased (≥40 g/l), this phase almost disappeared. This indicated that use of an appropriate NaOH concentration ensured more complete decomposition of hydrogarnet and improved alumina recovery. This was consistent with the results shown in Figure 7.

Noticeably, a dawsonite phase [$NaAlCO_3(OH)_2$] appeared when the NaOH concentration exceeded 30 g/l and a sodalite phase [$Na_8Al_6Si_6O_{24}(OH)_2H_2O$] was found above 60 g/l NaOH. The formation of such phases results in loss of Al and reduces its solubility. As a result, the alumina recovery declined at high NaOH concentrations, as shown in Figure 7.

The main reaction of the carbonation process is:

$$3CaO{\cdot}Al_2O_3{\cdot}xSiO_2{\cdot}(6-2x)H_2O+(3-2x)CO_2 \rightarrow xCa_2SiO_4 + (3-2x)CaCO_3+2Al(OH)_3+(3-2x)H_2O. \quad (5)$$

NaOH transforms into Na_2CO_3 with CO_2 in the carbonation process:

$$2NaOH+CO_2 \rightarrow Na_2CO_3+H_2O. \quad (6)$$

The $Al(OH)_3$ product from reaction (4) is converted into dawsonite in the presence of $NaCO_3$:

$$Al(OH)_3+Na_2CO_3+0.5H_2O+aq \rightarrow 0.5Na_2O{\cdot}Al_2O_3{\cdot}2CO_2{\cdot}3H_2O+NaOH+aq. \quad (7)$$

The main reaction of the carbonation process is therefore promoted by the formation of dawsonite. Moreover, dawsonite in the system can also react with NaOH in the digestion process:

$$Na_2O{\cdot}Al_2O_3{\cdot}2CO_2{\cdot}nH_2O+4NaOH+aq \rightarrow 2NaAl(OH)_4 + 2Na_2CO_3+(n-2)H_2O+aq. \quad (8)$$

This may explain why the Al_2O_3 recovery rises under certain alkali conditions. Sodalite, which has higher Na and Al contents, will be generated with further increase in alkali concentration:

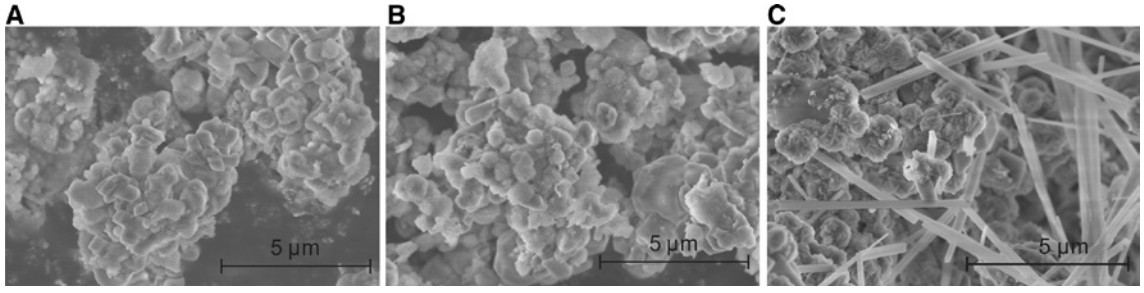

Figure 9: Scanning electron microscopy images of different carbonated residues. Morphologies produced by (A) the discrete process, (B) the direct process, and (C) the whole process using 40 g/l NaOH.

$$3CaO\cdot Al_2O_3\cdot xSiO_2\cdot(6-2x)H_2O+3CO_3^{2-}+xNa^+ \rightarrow xNaAlSiO_4+3CaCO_3+4OH^-+(2-x)Al(OH)^{4-}. \quad (9)$$

The sodalite phase cannot be digested in the process.

3.4 Scanning electron microscopy results

Morphologies of carbonated residues produced by the discrete and direct carbonation methods are shown in Figure 9A and B, respectively. Comparison shows that the structures of the carbonated residues were very similar. After carbonation, the carbonated residues exhibits an approximately round morphology with particle size of approximately 5 μm and a compact surface. Combining these data with chemical compositional analysis and XRD phase analysis, it was concluded that the presence of the Na alkali residue, caused by the omission of the liquid–solid separation step in the direct carbonation method, does not affect the final product. Carbonated residue obtained using a solution of 40 g/l NaOH is shown in Figure 9C. The product of needle-like structures appeared in carbonated residues. The needle-like structures on the surface were identified as dawsonite.

4 Conclusions

The direct carbonation process simplifies the process flow, making the steps of calcification and carbonation continuous. This significantly reduces equipment requirements and energy consumption, and shortens the processing time. Bayer process red mud can therefore be processed in a low-cost harmless way. Under optimal experimental conditions, the Na_2O concentrations in final residues treated by the direct and discrete carbonation processes were 0.21 %wt and 0.15 %wt, respectively, and the alumina recoveries were 35.5% and 34.9%, respectively. XRD analysis proved that the products from both processes were mainly composed of calcium carbonate and calcium silicate. Decomposition of the calcified residue can be optimized at a certain alkali concentration. With the addition of 40 g/l NaOH, the alumina recovery was maximized at 40.5% and the residual Na_2O in the final residue was reduced to <1 %wt.

Acknowledgments: This research was financially supported by the Joint Funds of the National Natural Science Foundation of China (no. U1202274), the National Natural Science Foundation of China (no. 51204040), Fundamental Research Funds for the Central Universities (N130702001), the Research Fund for the Doctoral Program of Higher Education of China (no. 20120042110011), and the Fundamental Research Funds for the Central Universities (no. N140204015).

Conflict of interest statement: The authors declare that there is no conflict of interest regarding the publication of this article.

References

[1] Zhu XF, Zhang TA, Wang YX, Lv GZ, Zhang WG. *Int. J. Miner. Metall. Mater* 2016, 23, 257–268.
[2] Leonardou SA, Oustadakis P, Tsakiridis PE, Markopoulos C. *J. Hazard. Mater* 2008, 157, 579–586.
[3] Nan XL, Zhang TA, Liu Y, Dou ZH. *Chin. J. Process. Eng.* 2010, 10, 264–270.
[4] Power G, Gräfe M, Klauber C. *Hydrometallurgy* 2011, 108, 33–45.
[5] Liu WC. [Dissertation]. Huazhong University of Science and Technology, Wuhan, 2010, p. 9.
[6] Klauber C, Gräfe M, Power G. *Hydrometallurgy* 2011, 108, 11–32.
[7] Tsakiridis PE, Leonardou SA, Oustadakis P. *J. Hazard. Mater*. 2004, 116, 103–110.
[8] Qin S, Wu BL. *J. Hazard. Mater*. 2011, 198, 269–274.
[9] Tor A, Danaoglu N, Arslan G, Cengeloglu Y. *J. Hazard. Mater*. 2009, 164, 271–278.
[10] Gray CW, Dunham SJ, Dennis PG, Zhao FJ, McGrath SP. *Environ. Pollut*. 2006, 142, 530–539.
[11] Liu WC, Sun SY, Zhang L, Jahanshahi S, Yang JK. *Miner. Eng*. 2012, 39, 213–218.
[12] Li XB, Xiao W, Liu W, Liu GH, Peng ZH, Zhou QS, Qi TG. *Trans. Nonferrous Met. Soc. China* 2009, 19, 1342–1347.
[13] Zhong L, Zhang YF, Zhang Y. *J. Hazard. Mater.* 2009, 172, 1629–1634.
[14] Zhang TA, Zhu XF, Lv GZ, Pan L, Liu Y, Zhao QY, Li Y, Jiang XL, He JC. *Light Met.* 2013, 233–238.
[15] Lv GZ, Zhang TA, Zhu XF, Pan L, Qin MX, Liu Y, Zhao Q, Jiang XL, Li Y. *Light Met.* 2013, 245–250.
[16] Zhu XF, Zhang TA, Lv GZ, Liu Y, Zhao QY, Li Y, Dou ZH. *Light Met.* 2013, 239–244.
[17] Li RB, Zhang TA, Liu Y, Lü GZ, Xie LQ. *J. Hazard. Mater.* 2016, 316, 94–101.
[18] Lv GZ, Zhang TA, Zhu XF, Liu Y, Wang YX, Guo FF, Zhao QY, Zheng CZ. *J. Oral. Micobiol.* 2014, 66, 1616–1621.
[19] Zhao QY, Zhu XF, Lv GZ, Zhang ZM, Yin ZN, Zhang TA. *J. Oral. Micobiol.* 2016, 68, 1711–1716.
[20] Zhu XF, Zhang TA, Lü GZ, Liu Y, Zhao QY. *Light Met.* 2013, 239–244.
[21] Li RB, Zhang TA, Liu Y, Zhou JP, Zou SK. *Powder Technol.* 2017, 311, 66–76.
[22] Melinda F, Lászlo K, György D, Richard VJ, Ferenc D. *Green Process. Synth.* 2016, 5, 239–246.
[23] Naveen KV, Prateek K, Nishith V. *Green Process. Synth*. 2015, 4, 37–46.
[24] Rivas Mercury JM, Penna P, Aza AHD, Turrillas, Sobrados I, Sanz J. *Acta Mater*. 2007, 55, 1183–1191.